Impact of annealing treatments on the softening and work hardening behaviour of Jethete M152 alloy for subsequent cold forming processes

Marcos Perez*

Advanced Forming Research Centre, University of Strathclyde, 85 Inchinnan Drive, Inchinnan, Renfrew PA4 9LJ.

*Corresponding author. Tel.: +44 (0) 141534 5524. marcos.perez@strath.ac.uk

ABSTRACT

Cold forming processes present advantages to produce components with tight tolerances to the final (net) shape, eliminating significant production costs. These processes requires forming parts in a soft condition, with high ductility and formability. Jethete M152 alloy is a cold formable 13-Cr% martensitic stainless steel used in the aerospace industry. However, the inherent high strength of this material presents challenges in terms of the high loads and contact and friction stresses developed during cold forming processes. The main purpose of this work was to explore the impact of different types of annealing treatments (subcritical, full and isothermal treatments) on the softening and work hardening behavior of this alloy. Microstructural and mechanical testing analysis were conducted. The results indicate that only subcritical annealing treatments ($T < A_{r1}$) were successful by reducing the strength and hardness levels. However no significant effect on both work hardening behavior and uniform elongation was found. Due to the high hardenability of this alloy, those softening treatments which require the austenization of the material were translated into the formation of freshly (as-quenched) martensite, resulting into an increase of strength, loss in ductility properties and a significant change in the work hardening behaviour. Despite of the large differences in strength properties and work hardening behaviour across all the softening treatments analyzed, no significant microstructural differences were found. These results indicate that such differences are associated mainly to both dislocation density and the substructure developed during tempering/annealing at high temperatures.

KEYWORDS

Jethete M152 alloy, annealing treatments, softening behaviour, work hardening, temper martensite.

1. INTRODUCTION

Cold forming methods present the advantages to produce components with tight tolerances to the final (net) shape, reducing the need of traditional finishing such as machining or grinding, and therefore, eliminating significant production costs. The application of these processes requires forming parts in a soft condition, with high ductility and formability, in order to accommodate the highest levels of deformation without failure. Jethete M152 alloy is a martensitic steel heat-resistant martensitic stainless steel, low C – high Cr alloy with additions of Ni and Mo, which exhibits and good weldability after forging, excellent fracture toughness. This alloy is employed in steam turbine components (blade and disc materials.) and compressor parts in gas turbine applications [1]. However, the inherent high strength of this material presents challenges in terms of the high loads required to introduce plastic deformation, as well as remarkable high contact and friction stresses developed during cold forming processes

Jethete M152 is is normalized (solution annealing for carbide dissolution) in an austenite regime, usually at 1,040–1,100°C, and then cooled to room temperature. The high Cr content (13% Cr) enables martensitic transformation during air cooling. The microstructure of low carbon high Cr hardened stainless is a combination of lath martensite, carbides and retained austenite among the laths. The substructure of lath martensite produced by quenching consists of high densities of tangled dislocations, reflecting lattice invariant deformation and volume accommodation effects during athermal transformation from high temperatures [2,3].

The as-quenched martensite is inherently brittle. Upon reheating at high temperature (tempering), the martensite will transform from the *bct* structure to a mixture of bcc iron and chromium carbides, leading to an increase in overall hardness (*secondary hardening*) [4]. With increase in the tempering temperature, the strength of the steel decreases significantly, but the toughness is largely improved and more stable. After tempering at high temperatures, both the lattice distortion and dislocation density in martensite is greatly reduced. However, tempered martensite is not a thermodynamically equilibrium phase; it evolves gradually during thermal ageing at high temperature. The most significant and obvious microstructural evolution is the recovery of martensitic lath, which has the strongest effect on strength. The martensitic lath recovery is a

process of dislocation movement and dislocation annihilation, resulting in migration of martensitic lath boundaries and formation of subgrains. The formation of subgrains is progressively developed by increasing temperature and plastic strains [4].

It is reported that the long-term stability of microstructure in 9–12 %Cr steels depends on the stability of precipitates, being the recovery processes correlated with the coarsening rate of chromium carbides [4]. For these steels, the subgrain boundaries are the main obstacles against the motion of dislocations. The migration of subgrain boundaries, causing the growth of subgrains, is closely correlated to the acceleration of the creep [4]. Hence, the subgrain boundary hardening is an important thermal stability mechanism. After the steel is aged at different temperatures for different times, coarsening of $M_{23}C_6$ carbides takes place by the mechanism of Ostwald ripening, resulting in a decrease of the pinning force due to $M_{23}C_6$ carbides with the subsequent coarsening of laths. Therefore, the main softening mechanisms of low carbon high Cr martensitic steels in tempered condition are expected to be both the reduction of dislocation density by means of recovery process and the coarsening of chromium carbides, losing the strengthening effect and reducing its role stabilizing the lath or subgrain of temper martensitic steels.

The purpose of this paper is to explore and understand the softening treatments and mechanisms involved in Jethete M152 alloy for subsequent (severe) cold forming process which requires maximum ductility and formability. A set of conventional and non-conventional annealing treatments, applied to martensitic stainless steels, were identified and conducted on Jethete M152 alloy supplied in tempered condition. The impact of annealing treatments on microstructure (SEM, EBSD) and mechanical properties (micro-hardness and mechanical testing) has been investigated.

2. EXPERIMENTAL WORK

2.1 Material Strategy

Jethete M152 bar with 110 mm in diameter was supplied in temper condition. Table 1 shows the chemical composition in as-supplied condition. Heat treatments were conducted in VFE/TAV TPH25/25/35 Horizontal Vacuum Furnace with an operating vacuum system at 10^{-4}-10^{-5} mbar.

Table 1. Chemical composition of Jethete M152 alloy

C	Si	Mn	S	P	Ni	Cr	Mo	V	Fe	N_2
0.11	0.22	0.68	0.0008	0.016	2.67	11.41	1.56	0.28	Compl.	0.026

2.2 Annealing treatments

Annealing is defined as the process whereby a material is heated to and held at a suitable temperature and then cooled at a well-defined rate to reduce hardness, improve the machinability, facilitate cold work, producing a specific microstructure, mechanical properties, etc. Basically, there are three types of annealing treatments applied to martensitic stainless steels [5]:

- Full annealing provides maximum softening by returning to the austenitic range, followed by slow cooling;
- Isothermal annealing is a heat treatment similar to full annealing treatment, but keeping the material isothermally at subcritical temperatures during certain periods of time; and,
- Subcritical annealing takes place in the upper portion of the ferritic range, just below the lower critical A_{c1} temperature.

Table 2 shows the type and treatment cycle of the first set of 6 heat treatments (HT). Based on the results of this first set, a second set were conducted in order to shed more light on the softening behaviour of Jethete M152. Table 3 describes the second set of heat treatments.

- The purpose of HT No.1, 2 & 9 (*subcritical annealing treatments*) was to explore the limits of softening of Jethete M152 alloy at subcritical temperatures (T = 700°C < A_{c1}) during increasing holding times: 6, 12 and 24 hours, respectively;
- HT No.3 (*full annealing treatment*) analyses the effect of austenization at 850°C followed by slow cooling rates;
- HT No.4 & 5 (*isothermal annealing treatments*), similarly to HT No.3, also explore the impact of austenization at 850°C, but holding isothermally the material at 720°C during 2 and 6 hours, respectively;
- The purpose of HT No. 8 is to understand the individual effect of low austenization temperatures on Jethete M152, by heating up to 850°C followed by fast cooling (air quenching);

- Finally, the main target of HT No.6, 9 & 10 (*isothermal annealing treatments*) is to transform isothermally the austenite to ferrite avoiding the martensitic transformation, but in this case, austenitising the material at higher temperatures (950 - 1050°C) and holding the material during long periods of time: 6, 12 and 24 hours, respectively.

Table 2. First set of Annealing treatments for Jethete M152 alloy

No.	Heat treatment	General description
1	Subcritical annealing	Heating to 700 °C - 6 hours + AC.
2		Heating to700 °C - 12 hours + AC.
3	Full annealing	Heating to 850°C – ½ hour+ slow cooling down to 540°C + AC.
4	Isothermal annealing	Heating to 850°C – ½ hour + slow cooling down to 720°C - 2 h + AC.
5		Heating to 850°C – ½ hour + slow cooling down to 720°C - 6 h + AC.
6		Heating to 1050°C – 1 hour + slow cooling down to 720°C - + AC.

Table 3. Second set of annealing treatments for Jethete M152 alloy

No.	Heat treatment	General description
7	Isothermal annealing	Heating to 950°C – ½ hour + 720°C - 12 hours + AC.
8	Full annealing	Heating to 850°C – ½ hour +fast cooling.
9	Subcritical annealing	Heating to 700 °C - 24 hours + AC.
10	Isothermal annealing	Heating to 1050°C – ½ hour + slow cooling down to 720°C - 24 hours + AC.

2.3 Microstructural and mechanical testing analysis

Microstructural analysis and mechanical testing were carried out in order to understand the impact of the softening treatments (Table 2, Table 3) on both microstructure and mechanical properties. The microstructure of the as-heat treated samples, including as-received condition, was investigated using scanning electron microscopy (SEM) and Electron Backscattered Diffraction technique (EBSD). The SEM instrument used was a high-resolution field emission type FEI / Oxford Instruments Quanta 250 FEG SEM, equipped with EBSD. EBSD scans of 160 μm × 140 μm were performed. A step size of 0.2 mm was selected in order to obtain

substructural information about lath martensite. The data analysis of EBSD scans was carried out by using CHANNEL 5 software.

In order to analyse the impact of softening treatments on mechanical properties, Vickers hardness measurements and tensile tests at room temperature were carried out. Zwick ZHV1 –micro Vickers hardness tester were used by applying a load of 2 kg (HV2). A minimum of 20 hardness measurements per sample were performed. For the first set of 6 heat treatments (Table 2), transverse sections of as received material (∅ 110 mm bar) were cut and heat treated subsequently. Tensile test specimens were obtained from the as-heat treated discs (∅110 × 32 mm) and machined in agreement with ASTM E8/E8M – 11. Subsize specimens with an overall length of 100 mm, a width of 6 mm and a thickness 3 mm were selected. Mechanical testing tests were conducted in Zwick/Roell Z150 Material Testing Machine by applying a strain rate control at speeds of 0.002 ± 0.001 /minute. Tensile strength, yield stress, uniform elongation, strain to fracture and area reduction were determined. At least, 2 tensile tests per condition were performed.

The work hardening rate (dσ/dε) and exponent values (n) were estimated from the yield to the ultimate tensile strength. The experimental true stress - true strain curves were fitted with the logarithmic form of Hollomon equation ($\sigma = k \cdot \varepsilon^n$):

$$\boldsymbol{ln\ \sigma = ln\ \ k + n\ ln\ \varepsilon} \qquad \textit{Equation 1}$$

where σ is the flow stress, k is the strength coefficient, ε is the plastic strain, and n is the work-hardening exponent. The instantaneous n-value and work hardening rate (θ) were obtained from experimental curves by the following equations:

$$\boldsymbol{n_i = \frac{d\ ln\ \sigma_i}{d\ ln\ \varepsilon_i} = \frac{\varepsilon_i}{\sigma_i}\frac{d\sigma_i}{d\varepsilon_i} = \frac{\varepsilon_i}{\sigma_i}\frac{(\sigma_{i+1}-\sigma_{i-1})}{(\varepsilon_{i+1}-\varepsilon_{i-1})}} \qquad \textit{Equation 2}$$

$$\boldsymbol{\theta_i = \frac{d\sigma_i}{d\varepsilon_i} = \frac{\sigma_i}{\varepsilon_i}n_i} \qquad \textit{Equation 3}$$

For this analysis, the differentiation of the true stress – true strain curve in needed, but the short-range noises may cause such differentiation calculus infeasible. In order to solve this problem, the curves were smoothed by plotting the average value of 20 consecutive data points.

3. RESULTS

3.1 Hardness analysis

The impact of annealing treatments on the mechanical properties of Jethete M152 alloy was analysed initially by means of hardness measurements (*HV2*). Figure 1 plots the hardness values of the 10 heat treatments (HT) analysed with respect to as-received condition, denoted by the black dotted line ($HV2_0$ = 339). For the subcritical annealing treatments (see Figure 2), a significant softening and a continuous drop in hardness was observed for HT No.1, 2 and 9 with holding times at 700°C of 6, 12 and 24 hours, respectively. From this figure, it is obvious the stronger softening effect during the first 6 hours, with a drop of $\Delta HV2$ = 37 kg/cm^2 (11%). However, the softening obtained during the subsequent holding time is more limited, with additional drop in hardness of 6 and 3% for HT No.2 and HT No.9, with holding times of 12 and 24 hours, respectively. These results denote a saturation effect on the softening behaviour of Jethete M152 alloy at subcritical temperatures ($T < A_{c1}$).

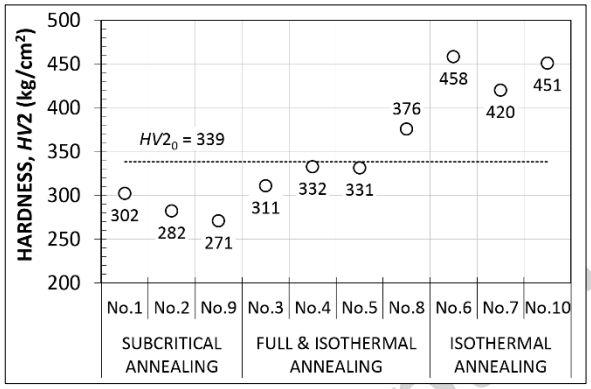

Fig. 1

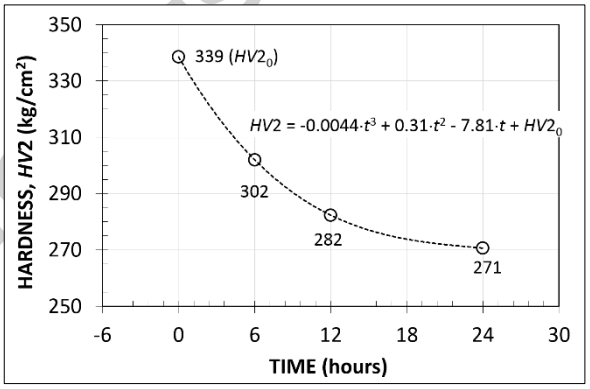

Fig. 2

Figure 1. Impact of the softening treatments (subcritical, full & isothermal) on hardness (HV2) against the hardness in as-received condition ($HV2_0$), denoted by the black dotted line.

Figure 2. Softening evolution as a function of holding time (hours) for subcritical annealing treatments: HT No.1, 2 and 9 with soaking times at 700°C of 6, 12 and 24 hours, respectively. The black circle ($HV2_0$ = 339) corresponds to the hardness in as-received condition.

The purpose of isothermal transformation treatments (No 6, 7 & 10) is to austenize the samples ($\alpha' \rightarrow \gamma$) at high temperature (1050°C) and then to cool down to 720°C, trying to transform isothermally the austenite to ferrite. However, instead of softening the material, the heat treatment No.6 (1050°C 1h + 720°C - 6h) presents

a sharp increase in hardness (458 HV2), corresponding, presumably, to the formation of virgin martensite (as-quenched). Similar results are obtained from heat treatment No. 7 (950°C ½h + 720°C - 12h) and No. 10 (1050°C ½h + 720°C - 24h) with hardness values of 420 and 451 HV2, respectively. These results highlight the remarkable hardenability of this alloy, avoiding the ferritic transformation ever after 24 hours of holding time at subcritical temperatures after austenization.

For full and isothermal annealing treatments which consist into heating up to 850°C and slow cooling to room temperature (HT No. 3) or holding at 720°C after austenization (HT No. 4 & 5), the softening obtained is far more limited in comparison with subcritical annealing treatments. As shown in Figure 1, only the heat treatment No.3 presents a significant drop in the hardness (311 *HV*2), in contrast with the HT No.4 & 5 which present levels of hardness (331 and 332 *HV*2 respectively) very close to that in as-received condition (339 *HV*2). In order to shed more light on these results, an additional heat treatment (HT No.8) was carried out in order to understand the individual effect of heating up to 850°C. In this case, the sample was air quenched (fast cooling) after being austenitized at 850°C. As shown in Figure 1, the hardness increases to 376 *HV*2, indicating that the reverse transformation from temper martensite to austenite ($\alpha' \rightarrow \gamma$) takes place with the subsequent formation of freshly martensite during the air quenching ($\gamma \rightarrow \alpha'$). Based on this result (HT No.8), the differences in hardness found between HT No.3 (311 *HV*2) *vs*. HT No. 4 & 5 (332 & 331 *HV*2) could be explained by the formation of softer phases during slow cooling to 540°C (HT No.3). However, no evidences were found in this respect. As will be commented later on, no significant differences in microstructure were detected across all the heat treated samples.

Figure 3 shows the effect of austenization temperature (850, 950 and 1050°C) on the hardness of HT No 6, 7, 8 & 10. From such figure, it is clear the strong effect of the austenization temperature on the final hardness, showing a linear dependency/relationship (R^2 = 0.99). These results are consistent with the expected increase in hardness due to the dissolution of larger amounts of chromium carbides ($M_{23}C_6$) in the matrix with increasing austenization temperatures. It is well known that the higher carbon supersaturation in the austenite prior to the martensitic transformation, the higher the lattice distortion of the martensite and the higher the amount of twin boundaries and dislocations in the microstructure will be [6-9].

Note that solution annealing treatment for Jethete M152 is usually applied at 1050°C in order to dissolve the chromium carbides. Lower temperatures will be translated into undissolved carbides prior to quenching. Therefore, the hardness results from full and isothermal heat treatments can be explained by the effect of austenization temperature on dissolution of the chromium carbides, increasing the carbon and chromium content in the matrix, and therefore increasing both the hardenability and the strength of the martensite by decreasing Ms. The increase in hardenability at high temperatures can explain the little or no effect of holding time at 720°C for isothermal treatments (HT No.6 & 10). In contrast, the lower hardenability at 850°C could also explain the differences between full (HT No.3) and isothermal annealing treatments (HT No 4 & 5).

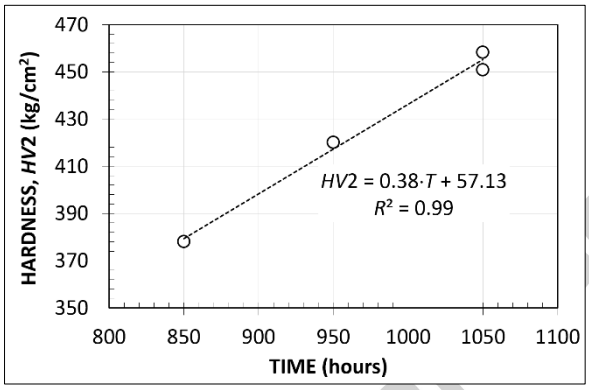

Figure 3. Impact of austenization temperature (850, 950 & 1050 °C) on hardness (HV2) for isothermal transformation treatments

3.2 Microstructural analysis (EBSD)

Martensite characteristically forms with a high dislocation density compared with alliotriomorphic ferrite and thus a term for this strengthening is often incorporated. The martensite laths, separated by low misorientation angle boundaries, are arranged in packet or colonies, separated by high angle boundaries. Figure 4 depicts the band contrast maps (BC) of Jethete M152 samples from two heat treatments (HT No.2 & 6) in direct comparison to the as-received condition. Despite of the large differences in mechanical properties (Figure 1) among these samples, no evident microstructural differences were observed.

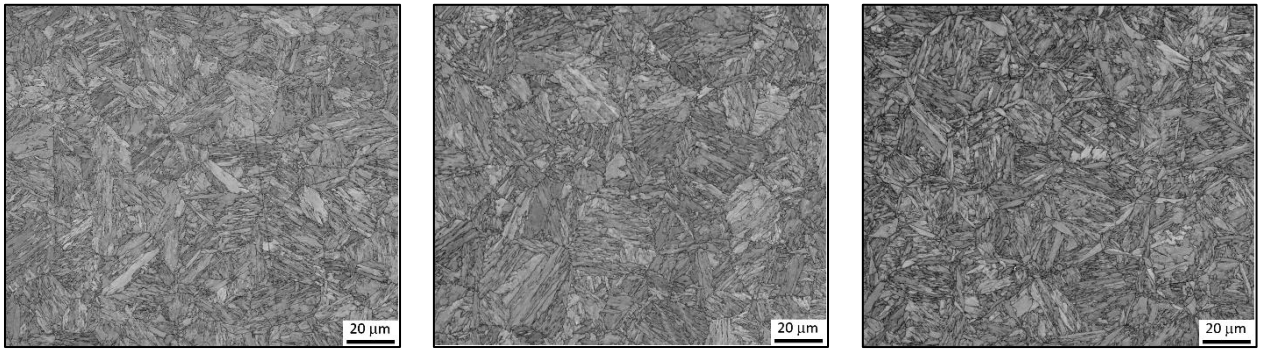

a) As-received (temper martensite) b) HT No.2 c) HT No.6

Figure 4. Band contrast maps (BC) of Jethete M152 specimens with band contrast maps ranging from 50 to 200 units.

Both the reduction of dislocation density inside the lath martensite and the increase of lath width due to recovery processes are softening mechanisms for low carbon high Cr martensitic steels. Based on this, the impact of softening treatments on block width was analysed by EBSD. The block width (l_i) was determined by using the Equation 4;

$$\boldsymbol{l_i} = \sqrt{\frac{4 \cdot A_i}{\pi \cdot (L/l)_i}} \qquad \text{EQUATION 4}$$

where A_i is the area and $(L/l)_i$ the aspect ratio of blocks, both calculated by CHANNEL 5 software by using a threshold misorientations of 2°. This equation assumes, as does CHANNEL 5 software, that the geometry/morphology of each grain is that of a fitted ellipse. Table 4 summarizes the statistical analysis of block distribution for all the heat treatments analysed in the present work, together with the hardness values discussed previously. From this table, an average block width in the range 1.1-1.3 mm was found for most of the cases. Only for subcritical annealing treatments, a slight increase of the block size was found with increasing holding time at 700°C, in agreement with the softening observed from hardness values (see Figure 2). For the rest of annealing treatments, due to presumably, the occurrence reverse transformation ($\alpha' \rightarrow \gamma$) and subsequent martensitic transformation ($\gamma \rightarrow \alpha'$), no relationship between block size and mechanical properties (HV2) were found.

Table 4. Block size of Jethete M152 heat treated samples

Lath/block size		l_{2°			HV2
		Mean	*Std. Error*	*Max.*	
As-received		1.090	0.591	7.566	339
Subcritical annealing	HT.1	1.214	0.621	8.259	302
	HT.2	1.241	0.653	7.540	282
	HT.9	1.342	0.766	11.690	271
Full annealing	HT.3	1.217	0.586	7.933	311
	HT.4	1.277	0.667	10.216	332
	HT.5	1.137	0.542	7.864	331
	HT.8	1.239	0.712	7.986	376
Isothermal transformation	HT.6	1.238	0.651	7.118	458
	HT.7	1.072	0.474	6.783	420
	HT.10	1.365	0.753	9.577	450

Another main effects of annealing treatments on tempered or annealed martensite is the reduction of dislocation density produced during the martensitic transformation giving place to significant amount of deformation to accommodate the shear stresses [10]. It is well known that elastic and plastic strain degrades the quality of diffraction patterns. With plastic strain, the distortions in the crystal lattice are relieved by the formation of dislocations, resulting pattern degradation, superposition of the patterns from each individual subgrain within the diffraction volume. The degree of degradation is dependent on the amount of deformation within the interaction volume. Therefore, the higher the dislocation density, the greater the degradation in pattern quality will be [10]. So, it is expected that those annealing treatments which provide the highest level of softening provide the maximum reduction on dislocation density and therefore the corresponding increase on patter quality for EBSD analysis [10].

For the present work, the impact of annealing treatments on band contrast (BC) and distribution of local misorientations were used in order to analyse the potential reduction in dislocation density during softening. Unfortunately, EBSD analysis were unsuccessful by detecting significant differences in strain distribution, not obtaining consistent results in direct comparison to those from hardness and tensile tests. Figure 5 plots the relative frequency of band contrast (BC) of heat treated samples which present large differences in mechanical properties. However, despite of such differences a similar BC distribution were observed. BS is not solely dependent on strain; other factors affect image quality as well, such as beam conditions, sample preparation, and camera settings [10]. Figure 7 plots the grain boundary distribution for subcritical annealing treatments (HT No.1,2,3 & 9) in direct comparison with as-received condition. As shown by this latter figure, all the curves are practically overlapped, not showing any difference for low angle boundaries distributions ($2° \leq LAGB \leq 15°$).

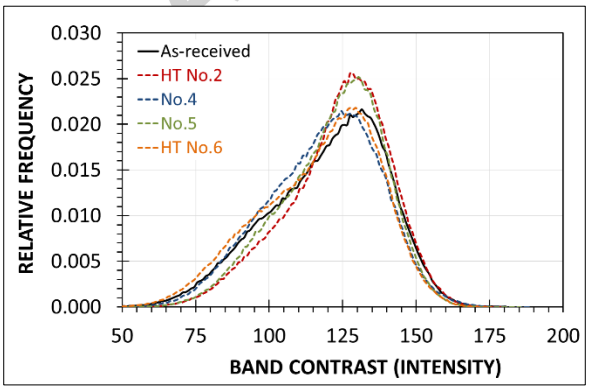

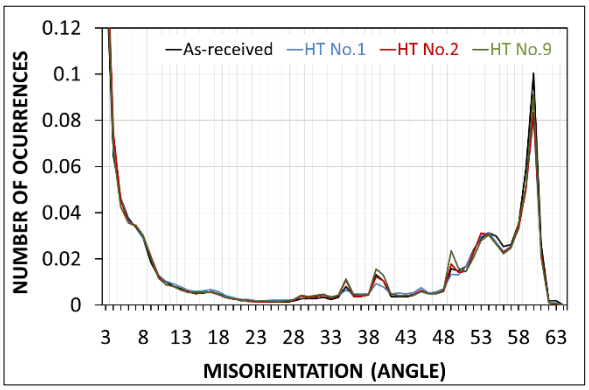

Figure 5 *Figure 6*

Figure 5. Relative frequency of Band contrast distribution for several Jethete M152 heat treated samples

Figure 6. Impact of subcritical annealing treatments on grain boundaries distributions

4. TENSILE TESTS

4.1 Engineering stress-strain curves

The engineering stress – engineering strain curves for the first six heat treatments (HT No.1 - 6) are plotted in Figure 7. In low carbon tempered martensite, the fine microstructure which control dynamic dislocation interactions during deformation consists of fine chromium carbides ($M_{23}C_6$) and the associated dislocation substructure and low angle boundaries (laths) [3]. From this figure, it is possible to observe that all the samples from the different softening treatments display continuous yielding, typical of martensitic microstructures.

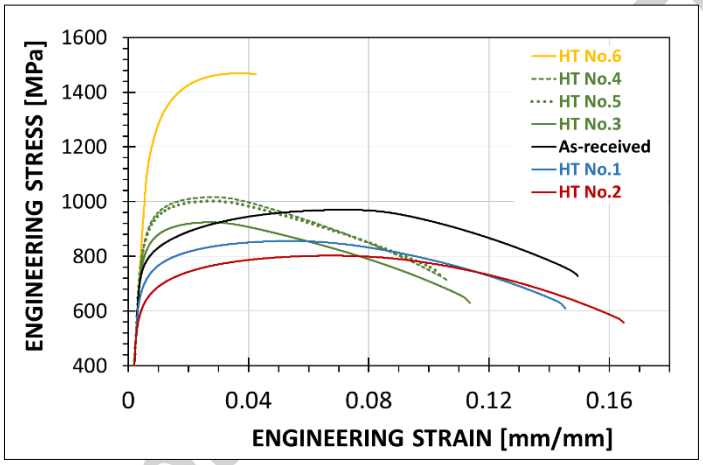

Figure 7. Engineering stress – engineering strain curves for three different types of softening treatments analysed (subcritical, full & isothermal and isothermal transformation annealing)

The engineering stress –strain curves from the subcritical annealing treatments (HT No.1 & 2) present significant similarities with that from as-received condition (Figure 7). Despite of the differences in strength levels, these curves present apparent similar work hardening behaviour and uniform elongation values. By contrast, full annealing (HT No. 3, 4 & 5) and isothermal treatments (HT No. 6) present a completely different behaviour. HT No.6 shows a high work hardening at low strains, but reaching a plateau with the occurrence of

the necking at much lower strains in comparison to both as-received condition and subcritical annealing treatments. For HT No. 3, 4 & 5 the post uniform strain is the major component of the total elongation.

Strength (yield stress, $\sigma_{0.2\%}$; ultimate tensile strength, σ_{Ult}) and elongations (ε_{Uni}, $\varepsilon_{Post\text{-}Uni}$) parameters calculated from the engineering stress – curves (Figure 7) are plotted in Figure 8 and Figure 9 with respect to as-received condition (*see dotted lines*). From these figures, it is evident the strong impact of the annealing treatments:

- *SUBCRITICAL ANNEALING (HT No.1 & 2)*: In agreement with hardness results (see Figure 1), subcritical annealing treatments provide a significant amount of softening. A remarkable drop in yield stress ($\sigma_{0.2\%}$) from 780 MPa (as-received) to 705 and 624 MPa, and from 970 MPa to 856 and 803 MPa in ultimate tensile strength (σ_{Ult}) is achieved for HT No.1 and No.2, respectively (Figure 8). Concerning elongation properties (Figure 9), the uniform elongation (ε_{Uni}), in contrast with the expected improvement from the drop of strength properties, presents a slight drop from 0.072 mm/mm (as-received) to 0.054 and 0.068 mm/mm for HT No.1 and No.2, respectively. In the case of post-uniform elongation (ε_{Post}), after necking, there is clear improvement from 0.078 (as-received) to 0.92 and 0.096 mm/mm for HT No.1 and No.2, respectively.
- *FULL & ISOTHERMAL ANNEALING (HT No.3,4 & 5)*: These annealing treatments were unsuccessful in softening the Jethete M152 alloy. The strength properties ($\sigma_{0.2\%}$, σ_{Ult}), with the exception of the ultimate strength of HT No.3, present slightly higher values than in as-received condition ($\sigma_{0.2\%}$ = 823 and σ_{Ult} = 925 MPa). The uniform elongation is drastically reduced from 0.072 mm/mm (as-received) to 0.027 mm/mm for all these heat treatments. However the post-uniform elongation is not affected in a significant manner, presenting similar figures to that in as-received condition ($\varepsilon_{Post\text{-}Uni}$ = 0.086, 0.079 & 0.077 mm/mm for treatments No.3, 4 & 5, respectively, $\approx \varepsilon_{Post\text{-}Uni,\ as\text{-}received}$ = 0.078).
- *ISOTHERMAL TRANSFORMATION (HT No.6)*: As commented previously, the remarkable high hardness of the heat treated sample from HT No.6 (456 HV2, Figure 1) clearly indicates that the microstructure consists into freshly martensite (as-quenched). The carbon content in solution largely determines the hardness and strength of low carbon as-quenched martensite and it is related carbon-dependent strengthening of the iron atom displacement caused by carbon atoms trapped in octahedral sides of the body-centred-tetragonal crystal structure [11]. Because of inherent high strength but also the brittleness

of as-quenched martensite, the corresponding tensile test curve (Figure 7) presents a remarkable increase in strength levels ($\sigma_{0.2\%}$ = 1212 MPa, σ_{Ult} = 1469 MPa) but with a sharp drop in strain to fracture. Note that the post-uniform elongation is only 7% of that in as-received condition, resulting into a brittle fracture after necking, as will be discussed later on. Despite the inherent brittleness (as-quenched condition) and the very high strength properties, HT No.6 presents a higher uniform elongation ($\varepsilon_{Uni\text{-}HT\ No.6}$ = 0.037 mm/mm) than those from HT No. 3, 4 & 5 (ε_{Uni} = 0.027 mm/mm).

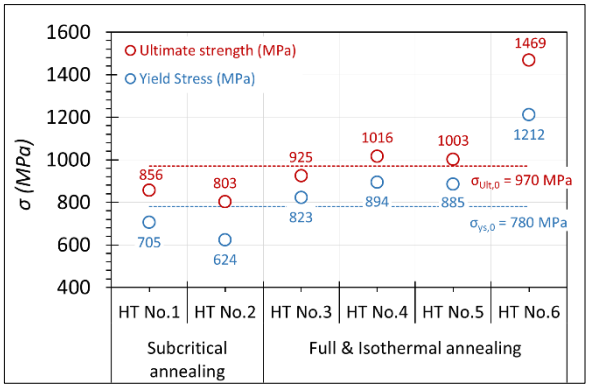

Figure 8

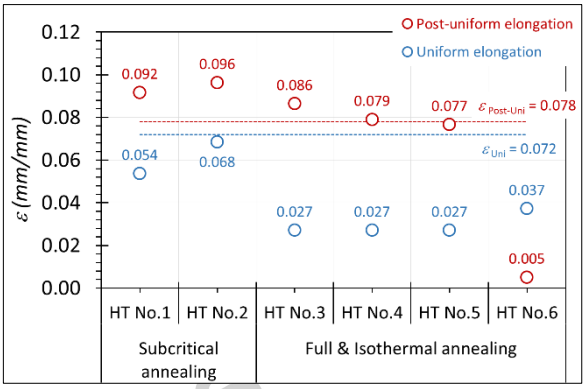

Figure 9

Figure 8.Yield stress and ultimate strength distributions

Figure 9. Uniform and post-uniform elongation distribution

The anomalous high uniform elongation of HT No.6 can be easily detected when the strength properties ($\sigma_{0.2\%}$, σ_{Ult}) are plotted versus elongation values (ε_{Uni}, $\varepsilon_{Post\text{-}Uni}$). As shown in Figure 10 and Figure 11, the increase in strength properties is generally accompanied by a drop in elongation properties. Figure 12 plots the strength values (σ_{ys}, σ_{Ult}) against hardness measurements (*HV*2), finding good linear correlations. Finally, Figure 13 shows how the amount of necking (reduction in area) and post uniform elongation are controlled by the ultimate tensile stress. Note that the higher the tensile stresses, the smaller/lower either necking or post uniform elongation are required to generate the triaxial stresses for final failure/fracture.

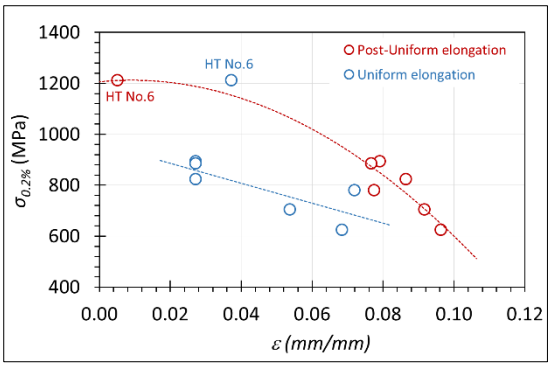

Figure 10

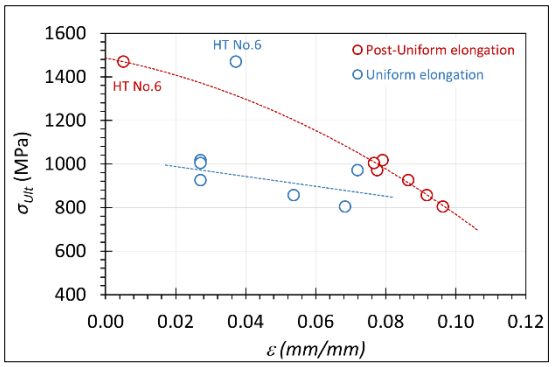

Figure 11

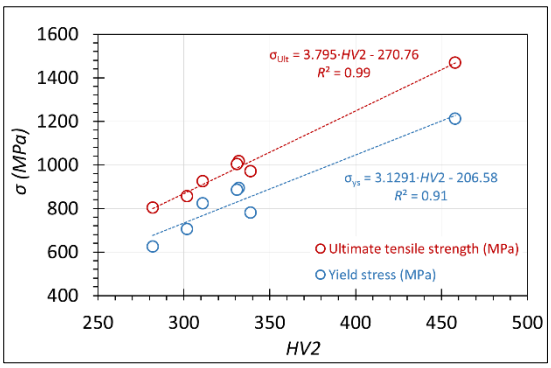

Figure 12

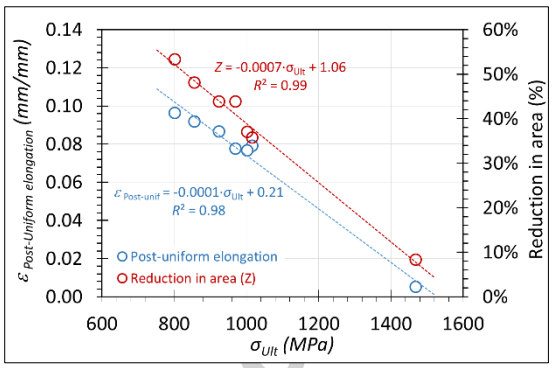

Figure 13

Figure 10. Relationships between yield stress and uniform & post-uniform elongation.

Figure 11. Relationships between ultimate tensile strength and uniform & post-uniform elongation.

Figure 12. Relationships between strength properties (σ_{ys}, σ_{Ult}) and hardness (HV2).

Figure 13. Relationships between ultimate tensile strength and both post uniform elongation (after necking) and area reduction.

4.2 Fracture surface

Figure 14 shows several examples of the fracture surface of tested tensile specimens from softening treatments. With the exception of the HT No.6, all the micrographs exhibit dimpled fracture surfaces as observed in Figure 14.a & b, characteristic in ductile fracture by the growth and coalescence of microvoids. The presence of carbide particles at the bottom of several dimples can be observed. In fact, the ductile fracture mechanism of these samples can be inferred from the engineering stress-strain curves (Figure 7) which exhibit a significant post-uniform elongation. The subcritical treatments (No.1 and 2) can be considered a prolongation of tempering treatment, in contrast with the full and isothermal heat treatments (HT No. 3, 4 & 5). The ductile fracture of these latter treatments could be explained by the inherent low strength and therefore the higher ductility of the martensite formed after austenitizing at low temperatures (850°C). Note

that the hardening treatments for Jethete M152 alloy is named solution annealing because its main purpose is dissolve the chromium carbides with an austenitization temperature as high as 1050°C. This temperature is around 200°C above conventional hardening treatment for low-carbon steels (≈ 820-870°C). So, the dissolution of very low amounts of chromium carbides are expected at temperatures as low as 850°C. This latter observation can also explain the nucleation and growth of voids on non-dissolved carbides for HT No3, 4 & 5.

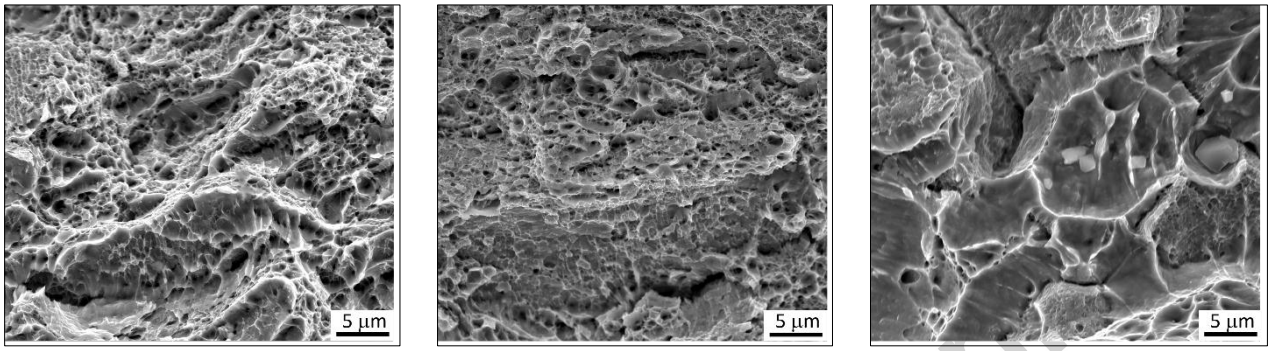

a) HT No.2 b) HT No.3 c) HT No.6

Figure 14. Fracture surface of Jethete M152 tensile tests.

On the other hand, the fracture surface of HT No.6 (Figure 14.c) shows a faceted fracture surface, characteristic of brittle cleavage fractures (intergranular), associated to the low post-uniform elongation value observed for this heat treatment (Figure 9). From Figure 14.c, it is remarkable the presence not only of coarse (non-dissolved) carbides in the matrix, but also the presence of voids in what seems to be prior austenitic grain boundaries. In this sense, Figure 15 shows SEM micrographs of the microstructure of HT No.6 at two magnifications. The etching response by using Villella's agent allows to identify the prior austenitic grain boundaries, see Figure 15.a. At higher magnifications (Figure 15.b) it is remarkable the precipitation, presumably, of chromium carbides on the (prior austenite) grain boundaries. Such massive grain boundary precipitation should have taken place in the curse of holding time at subcritical temperature (720°C) due to drop the chromium solubility in austenite after the dissolution of large fractions of chromium carbides at high austenization temperatures (1050°C). The embrittlement due to the presence of chromium carbides decorating the grain boundaries could also explain, in part, the brittle behaviour of HT No.6.

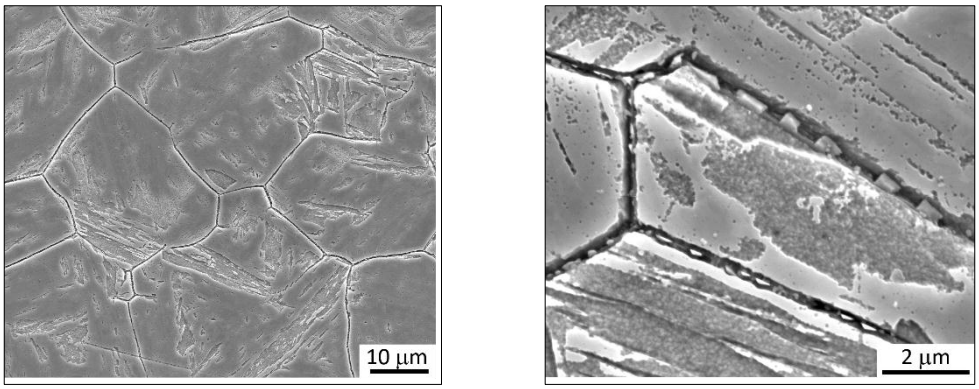

a) b)

Figure 15. a) Prior austenite grains with partially revealed lath-structure of Jethete M152 austenized at 1050 ℃ during 1 hour, and, b) Plate-like carbides precipitated along prior austenite grain boundaries.

4.3 Work hardening behaviour

In order to evaluate the impact of softening treatments on the work hardening behaviour of Jethete M152 alloy, both the Hollomon and instantaneous work hardening analysis were carried out.

Hollomon analysis

The strain hardening exponent (*n*) in the stress-strain relationship of metals and alloys is an indicator of their stretchability during press forming operations. The larger the *n* value, the more the material can deform before instability, and the material can be stretched further before necking starts [13]. The flow behaviour of the most metals and alloys can be described by Hollomon equation (Equation 1). A high strength coefficient (*k*) indicates a high initial resistance to plastic flow. Work hardening (*n*) is a measure of how the resistance to plastic flow increases as the metal is deformed [14]. Both *k* and *n* are affect not only by chemistry, but also by prior history and microstructure [13] and therefore, by heat treatment**.**

Figure 16 shows the ln true stress (ln σ) versus ln true strain (ln ε) for strains above the yield stress and Figure 17 plots both the strength coefficient (*k*) and the work hardening exponent (*n*) calculated for the first 6 heat treatments. From this latter figure, when compared with as–received condition (dotted lines), it is observed that most of the heat treatments reduce the work hardening exponent, with the exception of HT No.2 and 6. Concerning the strength coefficient, HT No.2 present the lowest value (*k* = 1175) in contrast with HT No.6 (*k* = 2399). It is found very often that higher work hardening coefficients create higher dynamic flow stresses and eventually resulting in increased uniform elongation. This latter on is agreement with the results observed in

igure 18. Despite the anomalous results from HT No.6, there is an increase of uniform elongation with increasing work hardening exponents.

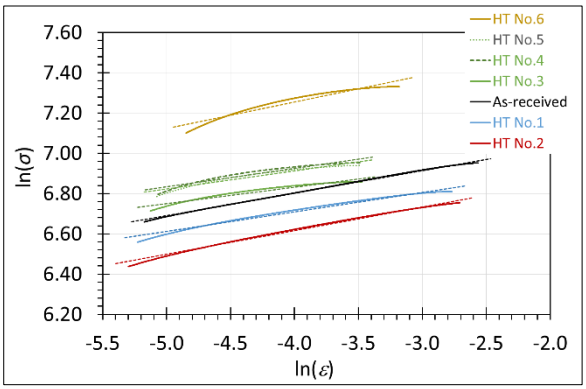

Figure 16

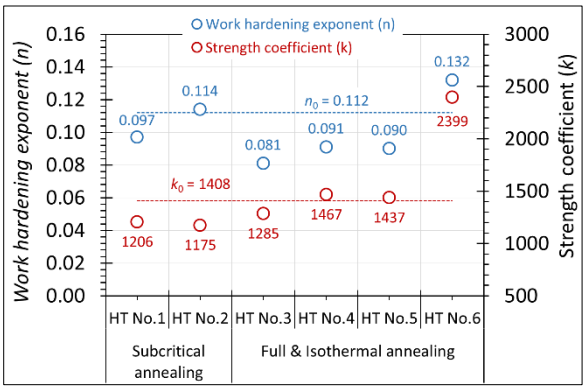

Figure 17

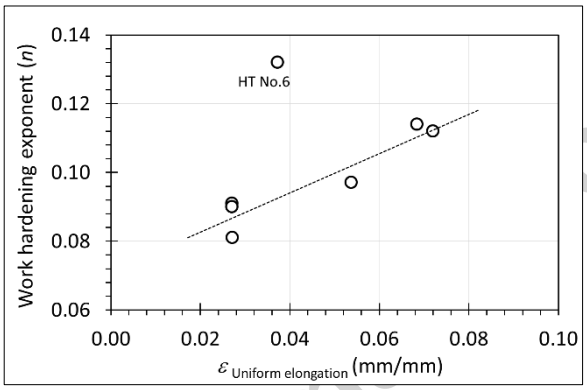

Figure 18

Figure 16. log true stress – log true strain curves of the first six heat treatments for work hardening coefficient calculation

Figure 17. plot of work hardening exponent (n) and strength coefficient (*k*)

Figure 18. Relationship between work hardening exponent (n) and uniform elongation (εUni)

As shown in Figure 16, as-received and subcritical heat treatments (HT No. 1 & 2) exhibit a power law hardening model which fits to the data as ln σ increases linearly with ln ε. The variation of log true stress with log true strain could indicate that the work hardening behaviour of this steel obeys a single stage work hardening mechanism. By contrast, for full and isothermal heat treatments (HT No.3,4,5 & 6), the ln σ increases nonlinearly with ln ε, therefore it seems that the Hollomon equation does not describe properly the work behaviour of these heat treatments. These latter results could indicate that the work hardening obey a two-stage work hardening mechanism, presenting a higher word hardening exponent at the first stage (at low strains), than that of the second stage. It is reported for dual phase steels (ferrite-martensite) non-linear

variation for ln σ with ln ε (multi stage work hardening mechanism) for high volume fractions of martensite [15].

Instantaneous strain hardening exponent (n) and work hardening rate (θ)

Additionally, the instantaneous strain hardening exponent (*n*-value) and work hardening rate (θ) were calculated by using Equation 2 and Equation 3, respectively, in order to further understand the work hardening behaviour of Jethete M152 alloy. The results from instantaneous *n*-values are plotted in Figure 19. It is obvious that maximum *n*-value (n_{max}) of Jethete M152 alloy, regardless the heat treatment applied, is reached immediately after the yield stress (σ_{ys}). Full and isothermal annealing treatments (HT No.3,4,5) exhibit the highest n_{max} values. This is attributed to the presence of fresh martensite (as-quenched) with higher dislocation density. With further straining, the different types of softening treatments develop a completely different work hardening behaviour. Full and isothermal annealing treatments present a sharp drop of instantaneous *n*-values and develop parallel curves until the occurrence of necking. Another aspect to be highlighted is that all the samples from full and isothermal annealing treatment austenitized at 850°C (HT No 3, 4 & 5) exhibit the same behaviour; basically the three curves are almost overlapped despite the significant differences of the heat treatments cycles. On the other hand, although the initial (instantaneous) *n*-values of both subcritical heat treatments (No.1 &2) and as-received condition are relatively small ($n < 0.20$), at a true strain range of 0.01 – 0.02 mm/mm, these curves develop a large plateau with a constant *n* value (flat curves). This results in a delayed necking at a larger strain, increasing the elongation values.

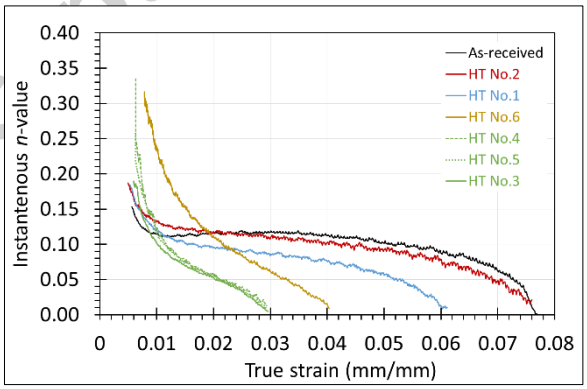

Figure 19

Figure 19. The variation of the instantaneous n-value with the true strain.

The variation of work hardening versus true strain is plotted in Figure 20 and Figure 21. Similar observations can be mentioned as those done for instantaneous *n*-values (Figure 19). From Figure 20 and Figure 21, high

work hardening rate during initial plastic deformation was observed for all the heat treatments. HT No.6 presents the highest work hardening ($d\sigma/d\varepsilon$) at low strains. With the increase of true strain, a marked reduction in work hardening was observed, developing parallel $d\sigma/d\varepsilon$ curves to HT No.3,4 & 5 in the late stage, as previously shown in Figure 19. The sharp drop in $d\sigma/d\varepsilon$ for both full and isothermal annealing treatments is in contrast with the gradual decrease of work hardening of subcritical treatments (HT No. 1 and 2) and as-received condition for true strains larger than 0.01 mm/mm (Figure 20).

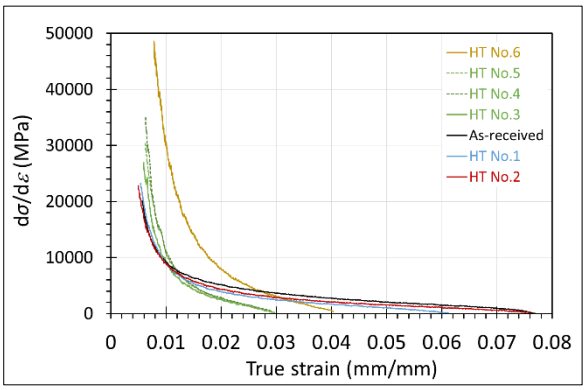

Figure 20

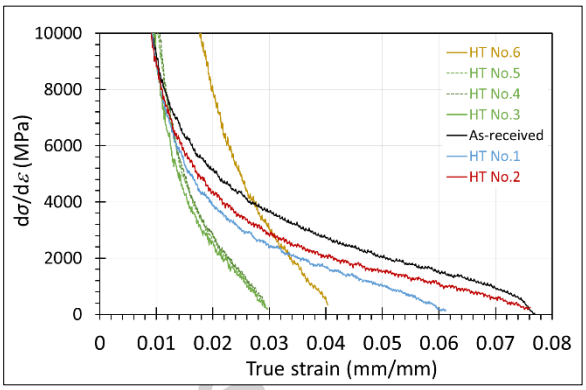

Figure 21

Figure 20. The variation of the work hardening rate (θ) with the true strain.

Figure 21. The variation of the work hardening rate (θ) against the true strain (zoom of Figure 20)

5. DISCUSSION

Based on the results from EBSD analysis, no significant microstructural differences were found across all the as-heat treated samples (see Table 4) despite of the large differences in strength properties and work hardening behaviour. It is reported that other microstructural parameters and strengthening mechanisms, besides the effective grain size, also have an important role in strength for martensitic steels: dislocation density, carbide precipitation, and martensitic substructure strengthening.

As-quenched martensite is well known to be strongest microstructure for a given steel composition, presenting a continuous yielding at low strain with rapid work hardening [16]. On the other side, tempering promotes the recovery of lath martensite by reducing its dislocation density and the coarsening of chromium carbides [4]. The larger dislocation density of as-quenched martensite is in good agreement with the higher work hardening rates observed at low strain for full and isothermal annealing treatments (HT No.3, 4, 5 & 6) in comparison with both subcritical annealing (HT No.1 & 2) and as-received condition (see Figure 20, Figure 21).

However, the remarkable differences found in work hardening behaviour among the softening treatments cannot be explained only by differences in dislocation density (as-quenched *vs*. temper martensite). Other microstructural features such as the initial martensite dislocation substructure, dislocation density evolution with strain, deformation substructure developed and the presence of chromium carbides can also be playing an important role on the work-hardening behaviour of Jethete M152 alloy.

Caron and Krauss [17] investigated the dislocation substructure of quenched and tempered Fe-0.2C martensitic steel samples, and they observed that the dislocation substructure in the tempered condition was much different compared to the as-quenched condition. Tempering at high temperature promotes the reorganization of the martensite dislocation substructure, developing dislocation cell structure and precipitation of chromium carbides on lath boundaries, but also the recovery of lath structure (reduction of dislocation density). In as-quenched condition, the dislocation network is essentially random (tangled dislocations). Due to the unpinned lengths of dislocation segments (mobile dislocations) and random dislocation network, the work hardening rapidly decreases due, hypothetically, to the motion of mobile dislocations. The authors found that at strains greater than 2%, the dislocation cell structure is well developed, similar to tempering, reorganizing the dislocation substructure. Within the cell structure, the spacing between the pinned segments of the dislocations is much shorter than that of as-quenched randomly tangled network. At strains greater than 2%, the dislocation cell structure is well developed and primarily controls the tensile properties.

In a similar fashion, the work hardening behaviour of full and isothermal annealing treatments (HT No.3, 4, 5 and 6) can be described as follows: The initial large work hardening values (Figure 20) are associated to the presence of as-quenched martensite with high dislocation density, being the differences between HT No3, 4 & 5 and HT No.6 associated to the austenization temperature (850 ad 1050°C, respectively). As commented before, higher austenization temperatures result into large difference in the dissolution of chromium carbides, as demonstrated by the hardness values (see Figure 3), increasing the carbon and chromium content in the matrix, and therefore increasing the strength of the martensite. With further strain, a dramatic and rapid change in work hardening slope takes place. Figure 22 plots the work hardening rate against true strains for HT No. 4 and 6, indicating the transition region from high work hardening rate at low strain to a critical strain where a stable and gradual decrease of $d\sigma/d\varepsilon$ is developed until necking. For HT No. 4 and 6 a critical strain of

1.6 and 2.2 % was estimated, respectively (see Figure 22). This critical strain could be associated to the development of a stable dislocation cell structure [11], in well agreement with the strain of 2% found by Caron and Krauss [17] for as-quenched Fe-0.2C martensite. This transition also could explain the observed two-stage work hardening behaviour from Hollomon's analysis (Figure 16) for full and isothermal annealing treatments.

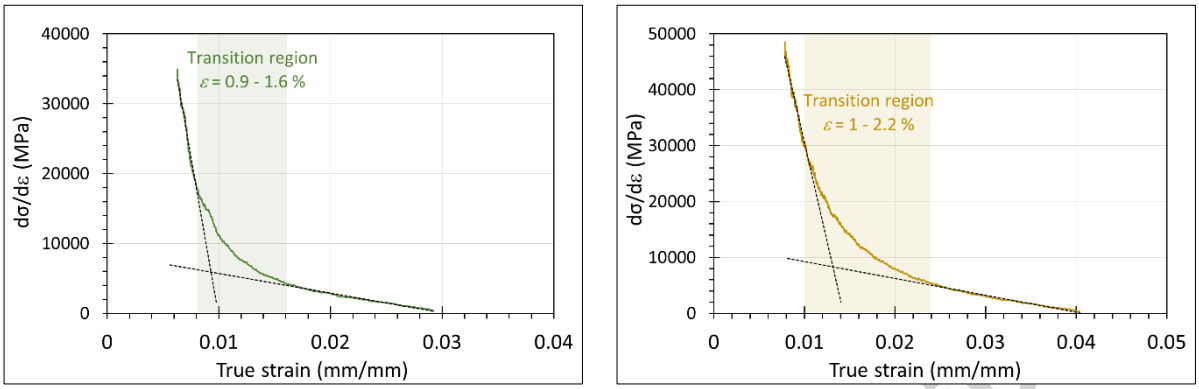

b) HT No. 4 *c) HT No.6*

Figure 22. The variation of the work hardening rate (dσ/dε) with the true strain

On the other hand, Caron and Krauss [17] also observed that high temperature tempering partially produces a dislocation cell network, similar to tensile deformation in the as-quenched condition. Similar to tensile deformation, tempering also promotes reorganization of the martensite dislocation substructure. The authors reported that after tempering at 400°C, a dislocation cell structure was developed. These findings are in good agreement with the work published by other authors. I. V. Gorynin *et al*. [18] analysed the impact of tempering in a secondary hardening steel (15KhN5M) at increasing temperatures. They observed that tempering at high temperature (650°C) the dislocation structure polygonises virtually fully. The dislocations form perfect stress-compensated dislocation nets and walls. The volume of elementary crystals of martensite breaks into polygonal cells with a characteristic size of 0.2 - 0.5 μm. At the same time special carbides coalesce intensely. A.Y. Kipelova *et al*. [19] studied evolution of dislocation structure in tempering of a high-chromium martensitic steel (10Kh9K3V1M1FBR) in the temperature range of 300 – 800°C. They observed that the structure of the steel tempered at 750°C experiences active redistribution of dislocations, rearranged into well discernible cells with a reduction of dislocation density. Therefore, for high temperature tempered samples, it seems that dσ/dε is primarily influenced by the dislocation cells formed during tempering at high temperatures.

In the present work, the smaller yield stress and initial work hardening rate observed for subcritical annealing treatments (HT No.1 & 2) could be related to their lower initial dislocation density. As shown in see Figure 23

for HT No.2, with further straining the work hardening rate decreases to a relatively constant rate over the entire stress-strain curve, retarding the occurrence of necking and increasing the uniform elongation. Note that this transition takes place at lower stress levels ($d\sigma/d\varepsilon$ < 11 kPa) and over a wider range of strain (HT No.2: 0.8-3 %) in comparison with full (HT No.4: 0.9 -1.6%, Figure 22.a) and isothermal annealing treatments (HT No.4: 1-2.2%, Figure 22.b). These results denote a more gradual transition of the work hardening behaviour for the as-tempered structures than for as-quenched ones. Therefore, the differences in both initial substructure (as-quenched vs. as-tempered), mainly, and dislocation density could explain the differences found in the work hardening behaviour for Jethete M152.

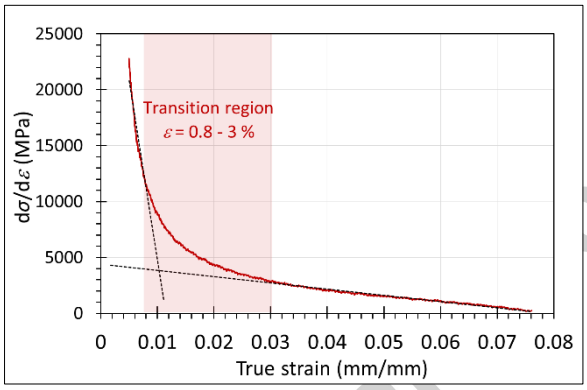

Figure 23. The variation of the work hardening rate (θ) with the true strain for HT No.2 (subcritical annealing treatment)

6. CONCLUSIONS

- Subcritical treatments ($T < A_{C1}$) provide significant softening to Jethete M152 alloy. The softening was accompanied by a slight increase of the block width, denoting the recovery of the lath structure. The engineering stress-strain curves are characterized by a continuous drop of strength properties with increasing holding time. However the ductility parameters and work hardening behaviour is not affected in a significant manner, exhibiting a similar behaviour as tempered martensite (as-received condition). The work hardening behaviour is characterized by both a large plateau with a constant *n*-value and a slight and gradual drop of $d\sigma/d\varepsilon$ curves along the uniform elongation region.

- The application of full and isothermal annealing treatments resulted into either no significant softening, or into a remarkable increase of both hardness and strength properties due to the formation of brittle martensite (as-quenched). The austenization temperature plays the most important role, finding a linear correlation between austenization temperature and hardness values.

This behaviour is associated to the dissolution of higher quantities of Cr-rich carbides at increasing temperatures. Due to the high hardenability of this alloy, heat treatment parameters, such as cooling rate and isothermal holding time, do not play a significant role in the softening and mechanical behaviour. The results from instantaneous *n*-values and work hardening rate show that the highest values are reached immediately after the yield stress, but presenting a marked drop with further strain and the occurrence of necking at low strains.

- The differences in both initial substructure (as-quenched vs. as-tempered), mainly, and dislocation density could explain the differences found in the work hardening behaviour among as-heat treated Jethete M152 specimens.

ACKNOWLEDGEMENTS

The work presented in this paper was funded by Innovate UK under SAMULET 2 Project 10.5 / Contract Ref TSB 113006. The author would like to acknowledge Rolls-Royce and the Advanced Forming Research Centre (AFRC) for their support in the project and help provided.

REFERENCES

[1] M.A. Alvarado-Meza, E. Garcıa-Sanchez, O. Covarrubias-Alvarado, A. Salinas-Rodriguez, M.P. Guerrero-Mata and R. Cola, Effect of the high-temperature deformation on the Ms temperature in a low C martensitic stainless steel, J. Mater. Eng. and Perform. Vol. 22(2) 345-350. (doi: 10.1007/s11665-012-0258-4).

[2] Martensitic structures, G.F. Vander Voort (Eds.), Metallography and Microstructures, ASM International, Vol.9 (2004) 165-178.

[3] K. Maruyama, K. Sawada and J. Koike, Strengthening mechanisms of creep resistant tempered martensitic steel, ISIJ Inter. Vol. 41 (2001) 641-653. (http://doi.org/10.2355/isijinternational.41.641).

[4] W. Yan, W. Wang, Y. Shan, K. Yang and W. Sha, 9-12Cr Heat Resistant Steels, Springer [Eds.] (2015).

[5] Heat treating of martensitic stainless steels, J. Dossett and G.E. Totten (Eds.), Heat treating of Iron and Steels, ASM International, Vol. 4D (2014), 397-417.

[6] A. Nasery Isfahanya, H. Saghafiana and G. Borhanib, The effect of heat treatment on mechanical properties and corrosion behavior of AISI420 martensitic stainless steel, J. Alloys & Comps. Vol. 509(9), 3931–3936. (http://dx.doi.org/10.1016/j.jallcom.2010.12.174)

[7] I. Calliari, M. Zanesco, M. Dabala, K. Brunelli and E. Ramous, Investigation of microstructure and properties of a Ni-Mo martensitic stainless steel, Material. & Design, Vol. 29(1) (2008) 246-250. (http://dx.doi.org/10.1016/j.matdes.2006.11.020)

[8] C. Garcia de Andres, G. Caruana and L.F. Alvarez, Control of $M_{23}C_6$ carbides in 0.45C-13Cr martensitic stainless steel by means of three representative heat treatment parameter, Mater. Sci. Eng. A Vol. 241(1-2) (1998) 211-215. (http://dx.doi.org/10.1016/S0921-5093(97)00491-7).

[9] A.F. Candelaria and C.E. Pinedo, Influence of the heat treatment on the corrosion resistance of the martensitic stainless steel type AISI 420, J. Mater. Sci. Letters Vol. 22(16) (2003) 1151–1153. (https://doi.org/10.1023/A:1025179128333).

[10] S.I. Wright, M.M. Nowell and D.P. Field, A review of strain analysis using Electron Backscatter Diffraction, Microsc. Microanal. Vol. 17 (2011) 316–329. (https://doi.org/10.1017/S1431927611000055)

[11] G. Krauss and D.K.Matlock, Effect of strain hardening and fine structure on strength and toughness of tempered martensite in carbon steels, J. Physique IV Colloque, Vol. 5 (1995) C8-51-C8-60. (http://dx.doi.org/10.1051/jp4:1995806).

[12] M. Mazinani and W.J. Poole, Effect of martensite plasticity on the deformation behaviour of a low-carbon dual-phase steel, Metall. Mat. Trans. A, Vol. 38(2) (2007) 328-339. (http://dx.doi.org/10.1007/s11661-006-9023-3).

[13] Bulk workability of metals, G.E. Dieter, H.A. Kuhn and S.L. Semiatin (Eds.), Handbook of workability and process design, (2003), 22-34.

[14] M.R. Akbarpour, A. Ekrami, Effect of ferrite volume fraction on work hardening behaviour of high bainite dual phase (DP) steels, Mater. Sci. Eng. A Vol.477(1-2) (2008) 306-310. (http://dx.doi.org/10.1016/j.msea.2007.05.051).

[15] X. Zuoa, Y. Chen and M. Wang, Study on microstructures and work hardening behaviour of ferrite-martensite dual-phase steels with high-content martensite, Mater. Research Vol. 15(6) (2012) 915-921. (http://dx.doi.org/10.1590/S1516-14392012005000118).

[16] G. Krauss, Martensite in steel: strength and structure, Mater. Sci. Eng. A, Vol. 273-275 (1999) 40-57. (http://dx.doi.org/10.1016/S0921-5093(99)00288-9).

[17] R.N. Caron and G. Krauss, The tempering of Fe-C lath martensite, Metal. Trans. Vol. 3(9) (1972) 2381-2389 (doi:10.1007/BF02647041).

[18] I.V. Gorynin, V.V. Rybin, V.A. Malyshevskii, T.G. Semicheva, and L.G. Sherokhina, Transformation of dislocation martensite in tempering secondary-hardening steel, Met. Sci. Heat Treat. Vol. 41(9) (1999) 377-383. (doi: 10.1007/BF02469875).

[19] A.Y. Kipelova, A.N. Belyakov, V.N. Skorobogatykh, I.A. Shchenkova, Tempering-induced structural changes in steel 10Kh9K3V1M1FBR and their effect on the mechanical properties, Met. Sci. Heat Treat. Vol. 52(3) (2010) 100-110. (doi: 10.1007/s11041-010-9240-7).